Journal of Theoretical and Applied Mechanics, Sofia, Vol.48 No.2 (2018) pp. 72-92
FLUID MECHANICS

MHD BOUNDARY LAYER FLOW OF NANOFLUID THROUGH A POROUS MEDIUM OVER A STRETCHING SHEET WITH VARIABLE WALL THICKNESS: USING CATTANEO–CHRISTOV HEAT FLUX MODEL

R.V.M.S.S. KIRAN KUMAR*, S.V.K. VARMA

Department of Mathematics, Sri Venkateswara University, Tirupati-517502, A. P, India

[Received 8 September 2017. Accepted 21 November 2017]

ABSTRACT: The hydromagnetic nanofluid flow over a stretching sheet in a porous medium with variable wall thickness in the presence of Brownian motion and thermophoresis is investigated. The heat transfer characteristics with variable conductivity are explored by using Cattaneo-Christov heat flux model. The governing non-linear ordinary differential equations are solved by using boundary value problem default solver in MATLAB bvp4c package. The impact of various important flow parameters on velocity, temperature and nanoparticle concentration as well as the friction factor coefficient and the rate of heat and mass transfer coefficients are presented and discussed through graphs and tables. It is found that the fluid velocity is accelerated with an increase in wall thickness parameter for $n > 1$, while the reverse trend is observed for $n < 1$.

KEY WORDS: Nanofluid flow; Magnetic field; Porous medium; Wall thickness parameter; variable thermal conductivity and molecular diffusivity.

1 INTRODUCTION

In recent years, the investigation of variable thickness stretching sheets with non-flatness is useful in the civil, marine, mechanical, aeronautical structure and designs etc. The variable thickness can be used to minimize the weight of structural elements. With this intention several researchers are attempt the flow problems by considering variable wall thickness stretching sheets.The study of stretching sheet flows with variable wall thickness has developed after the first study invented by Fang et al. [1]. The impact of temperature dependent viscosity and thermal conductivity on MHD flow over a stretching sheet with variable wall thickness was investigated by Anjali Devi and Prakash [2]. They found that the fluid properties like viscosity and thermal conductivity may gets vary at very high temperatures. Later, the influence of thermal radiation on MHD viscous flow over a slendering stretching sheet was considered

*Corresponding author e-mail: kksaisiva@gmail.com

by Anjali Devi and Prakash [3]. Furthermore, the hydromagnetic forced convective slip flow over a slendering sheet is considered by Anjali Devi and Prakash [4] and found that increasing wall thickness parameter causes to thinner thermal boundary layer structure.Vajravelu et al. [5] obtained the impact of Hall effects on hydromagnetic flow with variable fluid properties over a stretching sheet with variable wall thickness.Hayat et al. [6] studied the hydromagnetic nanofluid flow of a Powell-Eyring fluid over a stretching sheet with variable thickness and acknowledged that the higher values of velocity power index parameter enhances the surface drag coefficient. Further, Hayat et al. [7] analyzed the magnetic nanoparticles of tangent hyperbolic nanofluid over a stretching sheet with variable wall thickness and concluded that the velocity distribution decreases in terms of Weissenberg number and magnetic parameter.Kumar and Varma [8] investigated the magnetohydrodynamic nanofluid flow through porous medium over a slendering sheet under the influence of viscous dissipation, thermal radiation and chemical reaction and found that radiation parameter and thermophoresis parameter enhances the nanofluid temperature. Later, Kumar et al. [9] analyzed the hydromagnetic 3D slip flow over a slendering sheet by using single walled and multiwalled nanotubes. Recently, the non-linear MHD nanofluid flow with variable boundary-wall thickness is analyzed by Prasad et al. [10] and concluded that the flow decelerated with suction and accelerated with injection.

The temperature variations between two different bodies causes heat transfer mechanism. It plays an important role in the production of energy, cooling of nuclear reactors, biomedical applications for example heat conduction in tissues and drug targeting. Fourier [11] was originate the heat transfer phenomenon, which is parabolic energy equation for temperature field and has drawback that initial disturbance is felt instantly throughout the whole medium. So, Cattaneo [12] revised the Fourier law of heat conduction by adding the thermal relaxation term. This terms causes heat transportation in the form of thermal waves with finite speed. Furthermore, Christov [13] used the Oldroyd's upper convected derivative in place of time derivative in order to attain the material-invariant formulation. Therefore, this new model is known as Cattaneo–Chirstov heat flux model.The following researchers are analyzed the Cattaneo-Christov heat flux model in different geometries. Tibullo and Zampoli [14] examined the uniqueness of Cattaneo–Christov heat flux model for incompressible fluid flows.Han et al. [15] presented stretched Maxwell fluid flow with Cattaneo–Chirstov heat flux model. Shahid et al. [16] provided the influence of Cattaneo-Christov heat flux model on radiative Maxwell visco-elastic magnetized flow over a stretching permeable sheet.Mustafa [17] presented the Cattaneo–Christov heat flux model for Maxwell fluid over a stretching sheet and he concluded that velocity is inversely proportional to the visco-elastic fluid parameter. Moreover, fluid

temperature has inverse relationship with the relaxation time for heat flux and with the Prandtl number. The hydromagnetic flow of Williamson fluid over a slendering stretching sheet with Cattaneo–Chirstov heat flux model was proposed by Salahuddin et al. [18]. The impact of Cattaneo–Christov heat flux model on squeezing MHD nanofluid flow between two parallel plates with thermal radiation is considered by Dogonch and Ganji [19]. The flow of carbon nanotubes with chemical reaction over curved stretching sheet by using Cattaneo–Chirstov heat flux model was investigated by Hayat et al. [20]. The upper-convected Maxwell fluid flow over an exponentially stretching sheet using Cattaneo–Christov heat flux model is considered by Khan et al. [21]. Straughan [22] studied the thermal convection in an incompressible flow of upper converted Maxwell fluid by using Cattaneo–Christov model. The MHD 3D upper-convected Maxwell fluid flow over a stretching sheet with Cattaneo–Christov heat flux model is discussed by Rubab and Mustafa [23]. The hydromagnetic flow of a Casson fluid over a stretching sheet with variable wall thickness was analyzed by Malik et al. [24].

The aim of the present study is to investigate the hydromagnetic boundary layer flow of a nanofluid over a stretching sheet with variable wall thickness by using a new heat flux model namely; Cattaneo–Chirstov heat flux model. In this study, we consider the nanofluid thermal conductivity and species molecular diffusion coefficient are varying as linear factions of temperature and concentration. The resulting set of transformed equations is solved by using MATLAB bvp4c package. The influence of various important parameters are discussed and analyzed through graphs and tables.

2 MATHEMATICAL FORMULATION

We consider a steady two dimensional MHD flow of viscous incompressible and electrically conducting nanofluid in a porous medium bounded by a stretching sheet with variable wall thickness. Cattaneo–Chirstov heat flux model is used to investigate the heat transfer characteristics. It is assumed that the nanofluid thermal conductivity and species molecular diffusion coefficient is variable. The origin is located at the slit. The $x-$axis is chosen in the flow direction and the $y-$axis is normal to it (see Fig. 1). Let $u_w(x) = U_0(x+b)^n$ is the stretching sheet velocity (where U_0 is the constant, b is the physical parameter related to sheet and n is velocity exponent parameter). We assume that the present analysis is valid only for $n \neq 1$, since for $n = 1$ the problem reduces to a flat sheet. T_w and C_w are constant temperature and nanoparticle concentration, respectively. Buongiorno's model is incorporated to study the combined effects of thermophoresis and Brownian motion. A variable magnetic field $B(x) = B_0(x+b)^{(n-1/2)}$ acts in a transverse direction to the flow; also, the non-uniform permeability of the medium can be taken as the form $K = k'(x+b)^{1-n}$. We assume that the sheet is not flat and is defined as $y = A(x+b)^{(1-n)/2}$ $(n \neq 1)$

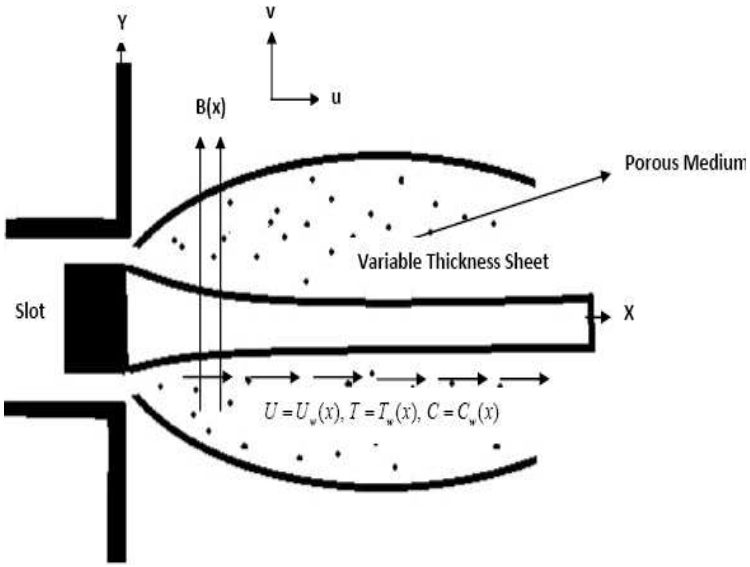

Fig. 1. Physical model and co-ordinate system.

(where A is chosen as very small constant. So that the sheet is adequately thin to avoid a measurable pressure gradient along the sheet (i.e. $\dfrac{\partial p}{\partial x} = 0$).

Under aforesaid assumptions, the governing boundary layer approximations can be written as (see [10] and [25])

$$\frac{\partial u}{\partial x} + \frac{\partial v}{\partial y} = 0, \tag{1}$$

$$u\frac{\partial u}{\partial x} + v\frac{\partial u}{\partial y} = \nu\frac{\partial^2 u}{\partial y^2} - \lambda_1\left(u^2\frac{\partial^2 u}{\partial x^2} + v^2\frac{\partial^2 u}{\partial y^2} + 2uv\frac{\partial^2 u}{\partial x \partial y}\right) - \frac{\sigma B_o^2(x)}{\rho}u - \frac{\nu}{k'}u, \tag{2}$$

$$\rho C_p\,(V \cdot \nabla T) = -\nabla \cdot q, \tag{3}$$

$$u\frac{\partial C}{\partial x} + v\frac{\partial C}{\partial y} = \frac{\partial}{\partial y}\left[D_B(C)\frac{\partial C}{\partial y}\right] + \frac{D_T}{T_\infty}\frac{\partial^2 T}{\partial y^2}, \tag{4}$$

we used a new flux model called as Cattaneo-Chirstov heat flux model and it has taken in the following form

$$q + \lambda_2\left[\frac{\partial q}{\partial t} + (V \cdot \nabla q) - (q \cdot \nabla V) + (\nabla \cdot V)q\right] = -k(T)\nabla T\,. \tag{5}$$

Here λ_2 for the relaxation time of heat flux, $k(T)$ for variable thermal conductivity which is linearly depends on fluid temperature. If $\lambda_2 = 0$ in Eq. (3), then the problem reduces to classical Fourier's law. Since the fluid is incompressible therefore Eq. (3) can be written as

$$q + \lambda_2 \left[\frac{\partial q}{\partial t} + (V \cdot \nabla q) - (q \cdot \nabla V) \right] = -k(T) \nabla T \,. \tag{6}$$

Comparing Eqs. (3) and (6) and eliminating q, we get the energy conservation law corresponding to Cattaneo-Chirstov heat flux model as follows:

$$\begin{aligned} u\frac{\partial T}{\partial x} + v\frac{\partial T}{\partial y} + \lambda_2 \Big(& u\frac{\partial u}{\partial x}\frac{\partial T}{\partial x} \\ & + v\frac{\partial v}{\partial y}\frac{\partial T}{\partial x} + u\frac{\partial v}{\partial x}\frac{\partial T}{\partial y} + v\frac{\partial u}{\partial y}\frac{\partial T}{\partial x} + 2uv\frac{\partial^2 T}{\partial x \partial y} + u^2\frac{\partial^2 T}{\partial x^2} + v^2\frac{\partial^2 T}{\partial y^2} \Big) \\ & = \frac{1}{\rho C_p}\frac{\partial}{\partial y}\Big[k(T)\frac{\partial T}{\partial y}\Big] + \tau\Big[D_B(C)\Big(\frac{\partial C}{\partial y}\frac{\partial T}{\partial y}\Big) + \frac{D_T}{T_\infty}\left(\frac{\partial T}{\partial y}\right)^2\Big], \end{aligned} \tag{7}$$

The variable thermal conductivity and variable molecular diffusivity are taken in the forms as [10,27]

$$k(T) = k_\infty \left(1 + \varepsilon_1 \theta\right), \tag{8}$$

$$D_B(C) = D_{B\infty}(1 + \varepsilon_2 \phi). \tag{9}$$

The associated boundary conditions are

$$\left.\begin{aligned} & u(x,y) = U_w = U_0(x+b)^n, \quad v(x,y) = 0, \\ & T(x,y) = T_w, \quad C(x,y) = C_w \end{aligned}\right\} \quad \text{at } y = A(x+b)^{\frac{1-n}{2}}, \tag{10}$$

$$u(x,y) \to 0, \quad T(x,y) \to T_\infty, \quad C(x,y) \to C_\infty, \quad \text{as } y \to \infty \,.$$

Here (u, v) denote the velocity components along $x-$ and $y-$directions, respectively. λ_1 is the relaxation time, ν is the kinematic viscosity, ε_1 and ε_2 are the variable thermal conductivity, variable species diffusivity parameters, respectively. θ is the dimensionless temperature, ϕ is the dimensionless concentration, k_∞, $D_{B\infty}$ are the ambient fluid thermal conductivity and Brownian diffusion coefficients, respectively. Also, D_T is the thermophoretic diffusion coefficient, τ is the heat capacity ratio, ρ is the nanoparticle density and Cp_f is the specific heat at constant pressure of the fluid.

3 SOLUTION OF THE PROBLEM

The suitable similarity variables are defined as follows.

Let ψ be the stream function which automatically satisfies the Eq. (1) and is given by

$$u = \frac{\partial \psi}{\partial y} \quad \text{and} \quad v = -\frac{\partial \psi}{\partial x}\,.$$

The appropriate similarity transformations are

$$\begin{aligned} &\psi(x,y) = f(\eta)\sqrt{\frac{2}{n+1}U_0\nu(x+b)^{n+1}}\,, \quad \eta = y\sqrt{\frac{n+1}{2}\frac{U_0}{\nu}(x+b)^{n-1}}\,, \\ &u = u_w f'(\eta)\,, \quad v = -\sqrt{\nu\frac{n+1}{2}U_0(x+b)^{n-1}}\Big[f(\eta) + \eta f'(\eta)\left(\frac{n-1}{n+1}\right)\Big], \\ &\theta(\eta) = \Big(\frac{T-T_\infty}{T_w-T_\infty}\Big), \quad \phi(\eta) = \Big(\frac{C-C_\infty}{C_w-C_\infty}\Big). \end{aligned} \tag{11}$$

By using the above similarity variables Eqs. (2), (4) and (7) and related boundary conditions (10) reduce to

$$\begin{aligned} &f''' + ff'' - \frac{2n}{1+n}f'^2 \\ &+ \beta\Big[(3n-1)ff'f'' - \frac{2n(n-1)}{1+n}f'^3 + \eta\frac{n-1}{2}f'^2f'' - \frac{(n+1)}{2}f^2f'''\Big] \\ &\qquad - (M+K)f' = 0 \end{aligned} \tag{12}$$

$$\begin{aligned} &(1+\varepsilon_1\theta)\theta'' + \varepsilon_1\theta'^2 + \Pr f\theta' \\ &\qquad + \Pr\,\gamma\Big[\frac{n-3}{2}ff'\theta' - \frac{(n+1)}{2}f^2\theta''\Big] \\ &\qquad\qquad + \Pr\, Nb(1+\varepsilon_2\phi)\phi'\theta' + \Pr Nt\theta'^2 = 0 \end{aligned} \tag{13}$$

$$(1+\varepsilon_2\phi)\phi'' + \frac{Nt}{Nb}\theta'' + Le\, f\phi' + \varepsilon_2\phi'^2 = 0. \tag{14}$$

The associated boundary conditions are

$$\begin{aligned} &f(\alpha) = \alpha\Big(\frac{1-n}{1+n}\Big), \quad f'(\alpha) = 1\,, \quad \theta(\alpha) = 1\,, \quad \phi(\alpha) = 1\,, \\ &f'(\infty) = 0\,, \quad \theta(\infty) = 0\,, \quad \phi(\infty) = 0\,. \end{aligned} \tag{15}$$

where α is a thickness parameter of the wall and η indicates the plate surface parameter, Pr is the Prandtl number, Le for Lewis number, Nb is the non-dimensional Brownian motion parameter, Nt is the non-dimensional thermophoresis parameter, M is the magnetic field parameter and x K is the permeability parameter, β is the Deborah number and γ is the thermal relaxation parameter.

Equations (12)-(14) with boundary conditions (15) are nonlinear differential equations with a domain $[\alpha, \infty)$. In order to assist the computation and change the domain to become$[0, \infty)$, we define $F(\xi) = F(\eta - \alpha) = f(\eta)$, $\Theta(\xi) = \Theta(\eta - \alpha) = \theta(\eta)$ and $\Phi(\xi) = \Phi(\eta - \alpha) = \phi(\eta)$.

In the view of above transformations Eqs. (12)-(15) become

$$
\begin{aligned}
(16)\quad & F''' + FF'' - \frac{2n}{1+n}F'^2 \\
& + \beta\Big[(3n-1)FF'F'' - \frac{2n(n-1)}{1+n}F'^3 + \eta\frac{n-1}{2}F'^2F'' - \frac{(n+1)}{2}F^2F'''\Big] \\
& \qquad - (M+K)F' = 0\,,
\end{aligned}
$$

$$
\begin{aligned}
(17)\quad & (1+\varepsilon_1\Theta)\Theta'' + \varepsilon_1\Theta'^2 + \mathrm{Pr}\,F\Theta' \\
& \qquad + \mathrm{Pr}\,\gamma\Big[\frac{n-3}{2}FF'\Theta' - \frac{(n+1)}{2}F^2\Theta''\Big] \\
& \qquad\qquad + \mathrm{Pr}\;Nb(1+\varepsilon_2\Phi)\Phi'\Theta' + \mathrm{Pr}\,Nt\Theta'^2 = 0\,,
\end{aligned}
$$

$$
(18)\qquad (1+\varepsilon_2\Phi)\Phi'' + \frac{Nt}{Nb}\Theta'' + LeF\Phi' + \varepsilon_2\Phi'^2 = 0.
$$

The related boundary conditions are

$$
\begin{aligned}
(19)\qquad & F(0) = \alpha\Big(\frac{1-n}{1+n}\Big), \quad F'(0) = 1\,, \quad \Theta(0) = 1\,, \quad \Phi(0) = 1\,, \\
& F'(\infty) = 0\,, \quad \Theta(\infty) = 0\,, \quad \Phi(\infty) = 0\,.
\end{aligned}
$$

The important physical quantities of interest are the friction factor coefficient (Cf_x), the rate of heat transfer coefficient (Nu_x) and the rate of mass transfer coefficient (Sh_x) are defined as

$$
\begin{aligned}
& Cf_x = \sqrt{2(n+1)}(Re_x)^{-1/2}F''(0)\,, \\
(20)\qquad & Nu_x = -[(n+1)Re_x/2]^{1/2}\Theta'(0) \quad \text{and} \\
& Sh_x = -[(n+1)Re_xt/2]^{1/2}\Phi'(0)\,,
\end{aligned}
$$

where $Re_x = U_w(x+b)/\nu$ is the local Reynolds number.

4 RESULTS AND DISCUSSION

The set of non-linear ordinary differential equations (ODE's) (12)-(14) with the boundary conditions (15) are solved by using boundary value problem default solver in MATLAB bvp4c package. The impact of various flow parameters are presented through graphs (2-15) and tables (1-2). Also, we compare the present results in the absence of λ, M, Nt, Nb, Le, K, ε_1, $\varepsilon_2\beta$, and γ with the obtained results of with the existing results obtained by Fang et al. [1], Prasad et al. [10] and Khader and Megahed [26]. For a typical nanofluid parameters Nb, Nt, varies between 0 to 1 and Le varies up to 20 (For details the reader may referrer [28]). A high Deborah number $(\beta \gg 1)$ represents solid-like behavior and low values $(\beta \ll 1)$ exhibit liquid-like behavior with respect to the observation time. The viscoelastic property dominates while β is in the range of 1. (For details see [29]). The Prandtl number for liquid metals is $\mathrm{Pr} \ll 1$ (For details the reader may referrer [30]). Moreover, for numerical calculation we fixed the values of dimensionless parameters as $\alpha = 0.5$, $\beta = 0.2$, $M = 2$, $\mathrm{Pr} = 0.71$, $\gamma = 0.1$, $\eta = 0.5$, $n = 1.5$, $\varepsilon_1 = 0.1$, $\varepsilon_2 = 0.1$, $Nt = 0.2$, $Nb = 0.3$, $Le = 1.5$, $K = 2$.

Fig. 2 elucidates the effect of magnetic field parameter (M) on $F'(\eta)$. It is noted that the improving values of M depreciates the fluid velocity. This is because increasing values of M develops the Lorentz forces which produce resistance to flow. Therefore, the velocity is decreases.In the physical view, the magnetic field parameter

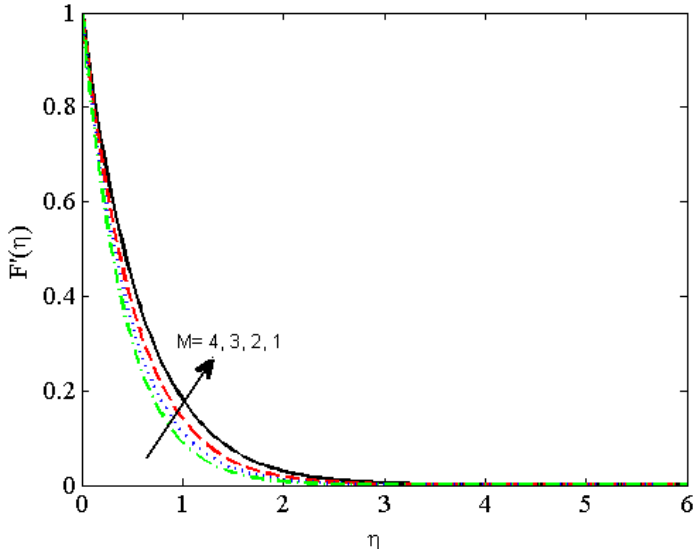

Fig. 2. Effect of M on $F'(\eta)$.

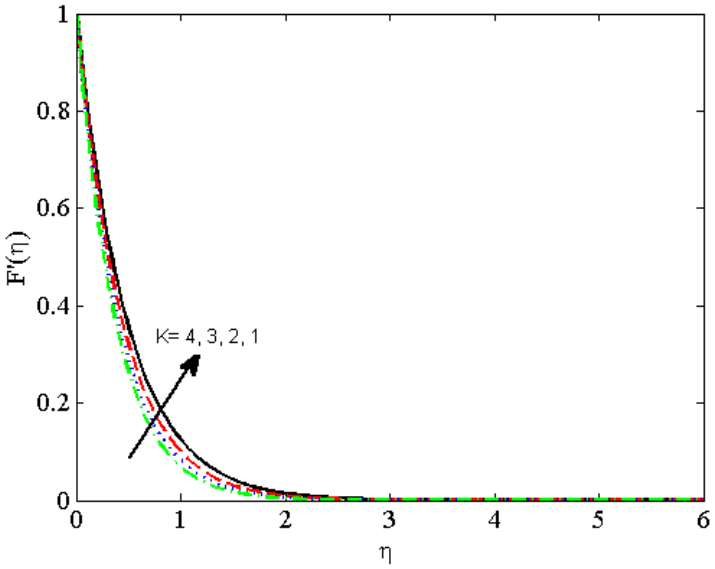

Fig. 3. Effect of K on $F'(\eta)$.

represents the ratio of magnetic force with the viscous force, so that the large value of M explicit the increase of Lorentz force. This is drag like force that produces more resistance to transport phenomena due to which fluid velocity reduces.

Fig. 3 shows the influence of porosity parameter (K) on $F'(\eta)$. It is seen that the velocity profiles are decreasing function of$K$. It is obvious that the presence of porous medium causes high limitations in fluid flow, which makes slow in its motion. Therefore, with increasing permeability parameter, the resistance to the fluid motion increases and hence velocity decreases.

Figs. 4-6 represent the effect of wall thickness parameter (α) on velocity, temperature and nanoparticle concentration fields. It is observed that the velocity, temperature and concentration and profiles are increasing function of α for $n > 1$, but reverse trend is observed for the case of $n < 1$. This is because from the boundary condition $F(0) = \alpha\left(\frac{1-n}{1+n}\right)$, for $n > 1$, we have $F(0) < 0$, i.e. mass injection and for $n < 1$ we have $F(0) > 0$, it represents mass suction at the wall. From these figures, it is observed that the flow is significantly decreases for suction while it is increases for injection. Further, all the three boundary layers thickness decreases for $-1 < n < 1$ but improved for $n > 1$.

Figs. 7 show the effect of power index parameter (n) on $F'(\eta)$. From this figure it is concluded that the hydromagnetic boundary layer thickness become thicker as

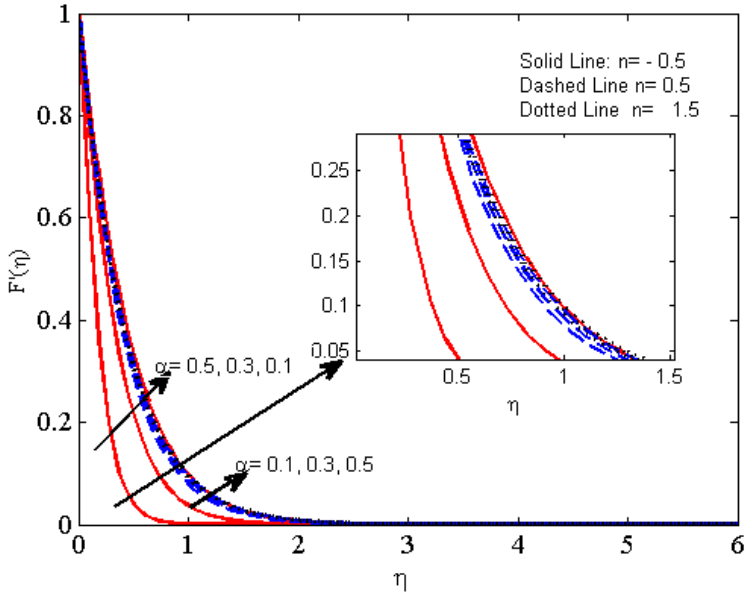

Fig. 4. Effect of α on $F'(\eta)$.

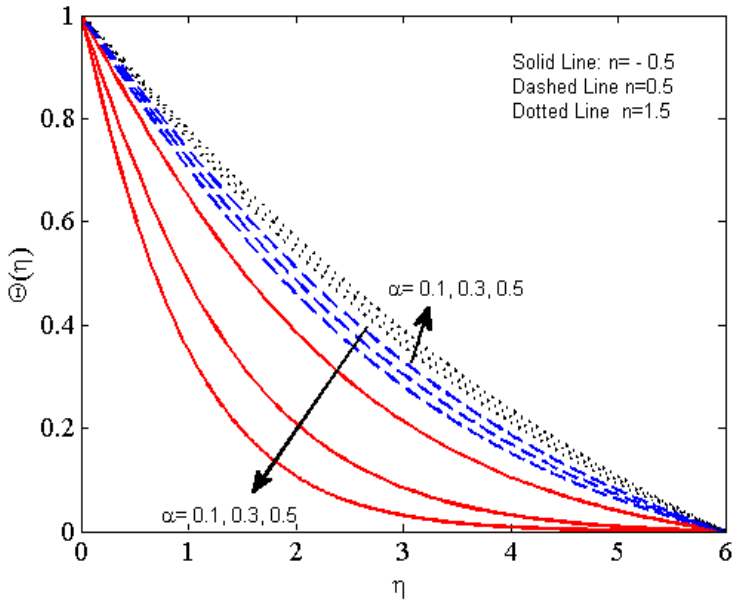

Fig. 5. Effect of α on $\Theta(\eta)$.

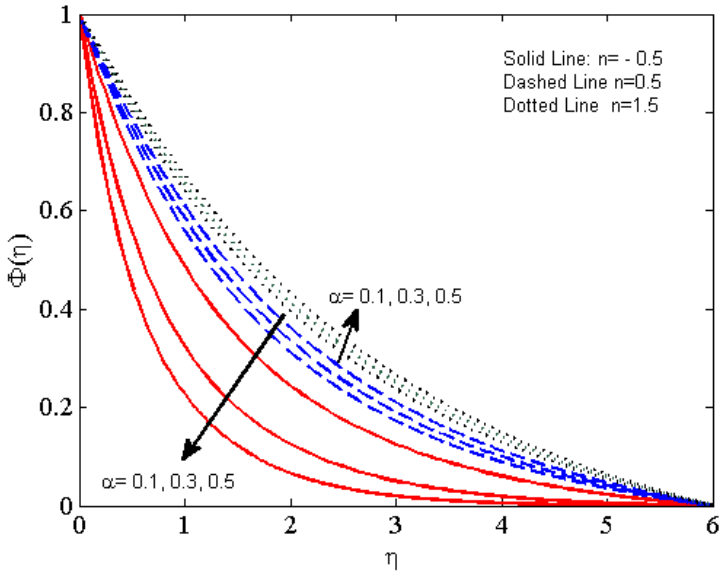

Fig. 6. Effect of α on $\Phi(\eta)$.

$n$increases along the sheet. This is due to the fact that higher values of n assist the fluid to slide faster over the surface which, in turn, makes the flow accelerate and the velocity boundary layer thickness increase. According to the nature of this problem, increase in velocity power index leads to slendering in the thickness of the sheet. This slenderness gives some boost to the flow velocity. The power index parameter has physical significations such that the parameter can controls the surface shape, kind of motion and the behavior of the boundary layer. It is clearly recognized that surface shape is profoundly relied on the numerical values of n such that the case of flat surface can be accomplished for $n = 1$ which has the constant thickness. For the occurrence of $n > 1$, the present study changed to surface whose thickness is reduced and for this situation a concave outer like surface shape will show up. Then again, if there should be an event of $n < 1$the surface has a convex outer shape and wall thickness is expanding. As we call 'n' to be the motion parameter, so this can control the type of motion. For $n = 0$ we have case of linear motion with constant velocity and $n > 1$compares to accelerated motion while $n < 1$ relates to decelerated motion.

The rising values of Brownian motion parameter (Nb) increases the nanofluid temperature, it is presented in Fig. 8. The reason behind the fact that more heat is generated for a nanofluid compared with a regular one and it leads to higher temperature. Whereas, the opposite trend is observed on $\Phi(\eta)$ (see Fig. 9). This figure

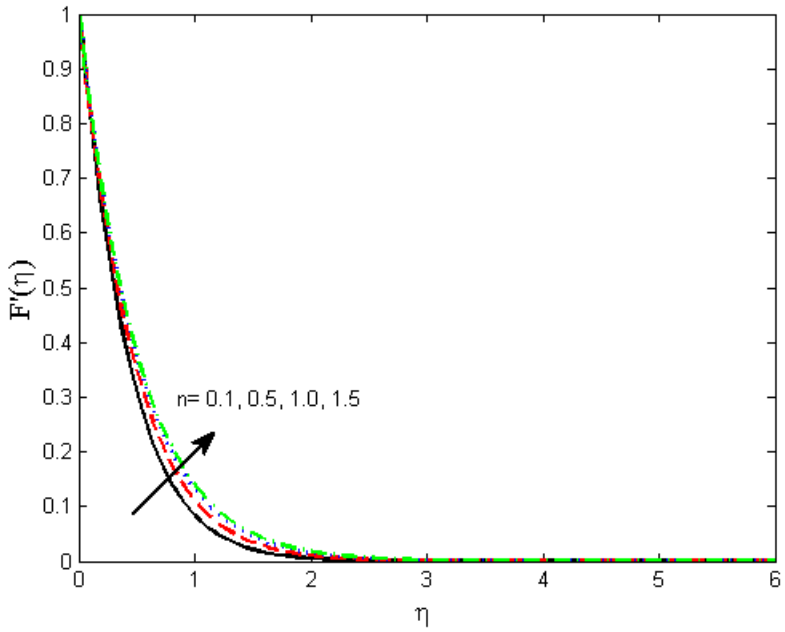

Fig. 7. Effect of n on $F'(\eta)$.

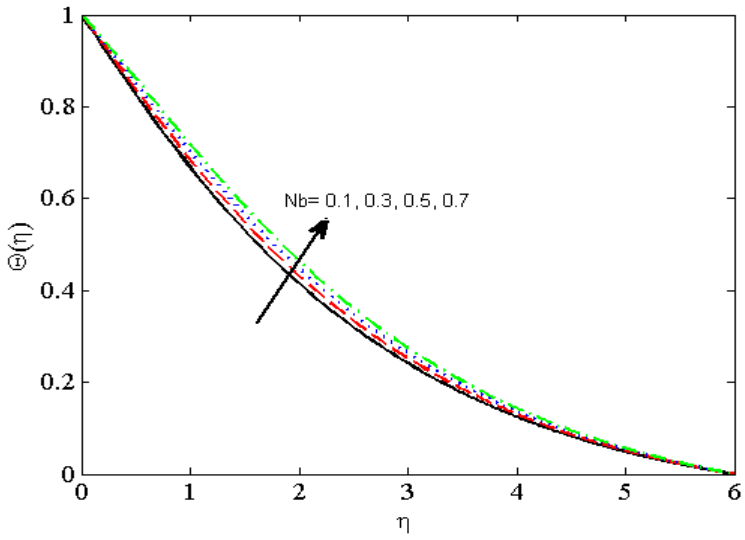

Fig. 8. Effect of Nb on $\Theta(\eta)$.

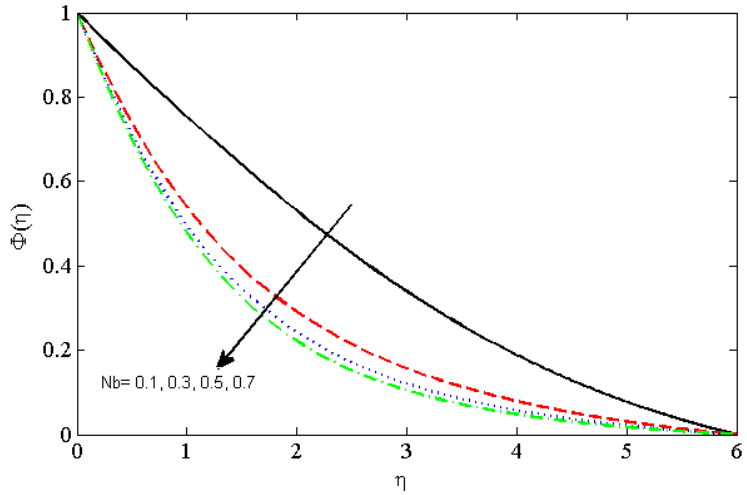

Fig. 9. Effect of Nb on $\Phi(\eta)$.

analyzes that lesser value of Nb leads to the thicker boundary layer thickness. It is interesting to note that the Brownian motion of nanoparticles at molecular and nanoscale levels are a key nanoscale mechanism governing their thermal behaviors. In nanofluid systems, due to the size of the nanoparticles, the Brownian motion takes place, which can affect the heat transfer properties. As the particle size scale approaches to the nanometer scale, the particle Brownian motion and its effect on the surrounding liquids play an important role in the heat transfer.

Figs. 10 and 11 reveal that the influence of thermophoresis parameter (Nt) on $\Theta(\eta)$ and $\Phi(\eta)$. As Nt increases the temperature and nanoparticle concentration profiles are enhanced within the boundary layer, therefore, we observed the development of thermal and concentration boundary layers thickness. It is clear that; positive Nt indicates a cold surface while negative to a hot surface. For hot surfaces, thermophoresis leads to blow the nanoparticle volume fraction boundary layer away from the surface since a hot surface repels the sub-micron sized particles from it, thereby forming a relatively particle-free layer near the surface. In particular, the effect of increasing the thermophoretic parameter Nt is limited to increasing slightly the wall slope of the nanoparticle volume fraction profiles, but decreasing the nanoparticle volume fraction. This is true only for small Lewis numbers for which the Brownian diffusion effect is large compared with the convection effect. However, for large Lewis numbers, the diffusion effect is minimal compared with the convection effect. Therefore, the thermophoretic parameter Nt is expected to alter the nanoparticle volume fraction boundary layer significantly.

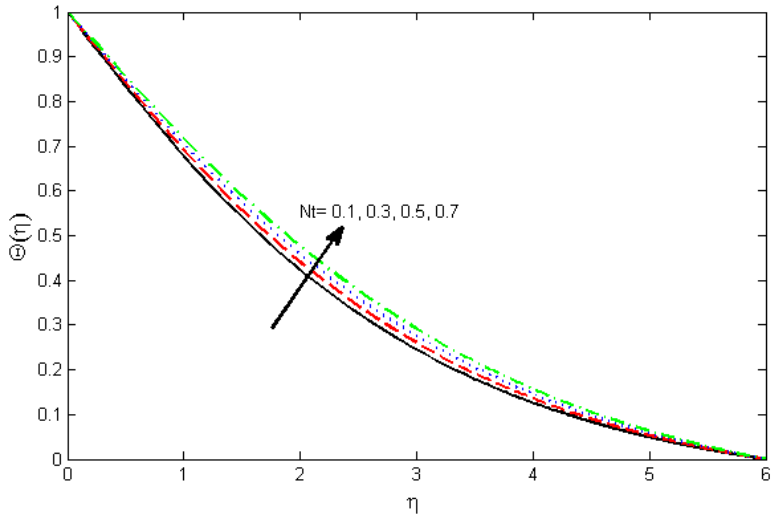

Fig. 10. Effect of Nt on $\Theta(\eta)$.

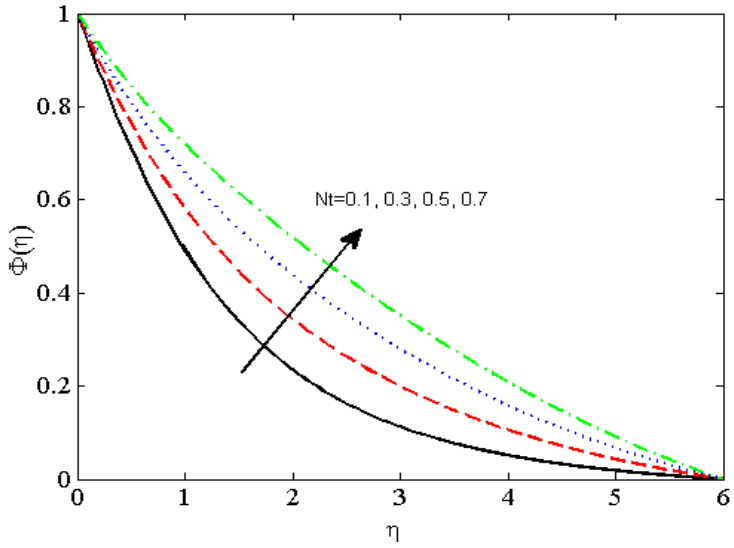

Fig. 11. Effect of Nt on $\Phi(\eta)$.

Fig. 12 displays the impact of thermal conductivity parameter (ε_1) on temperature filed. It is seen that the rising values of ε_1 causes to improve the fluid temperature. Physically, enhancement of thermal conductivity parameter leads to increase the thermal conductivity of the fluid. Therefore, more heat is transformed from sheet

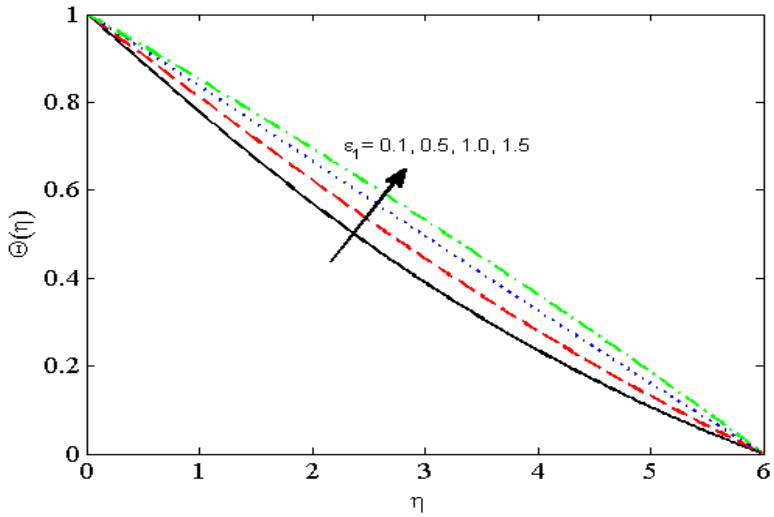

Fig. 12. Effect of ε_1 on $\Theta(\eta)$.

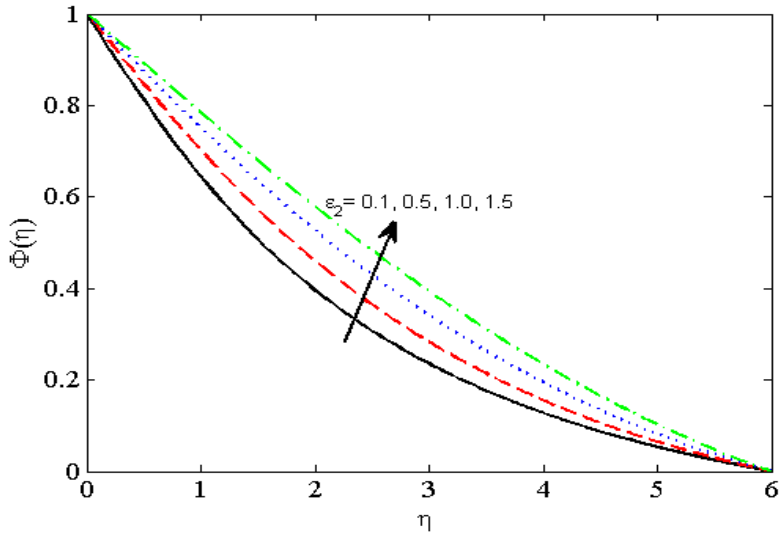

Fig. 13. Effect of ε_2 on $\Phi(\eta)$.

to the fluid. Hence the fluid temperature increases.The influence of species diffusivity parameter (ε_2) on nanoparticle concentration distribution is plotted in Fig. 13. It is evident that the larger values of ε_2 enhance the nanoparticle concentration and boundary layer thickness. This is because the species diffusivity is proportional to

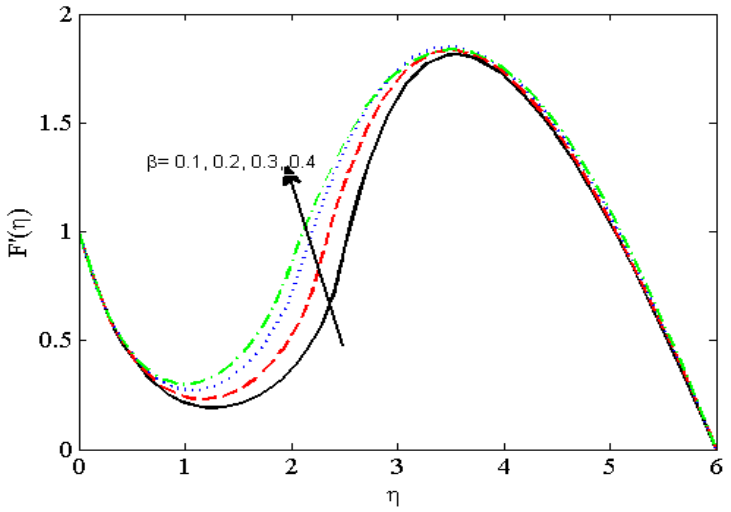

Fig. 14. Effect of β on $F'(\eta)$.

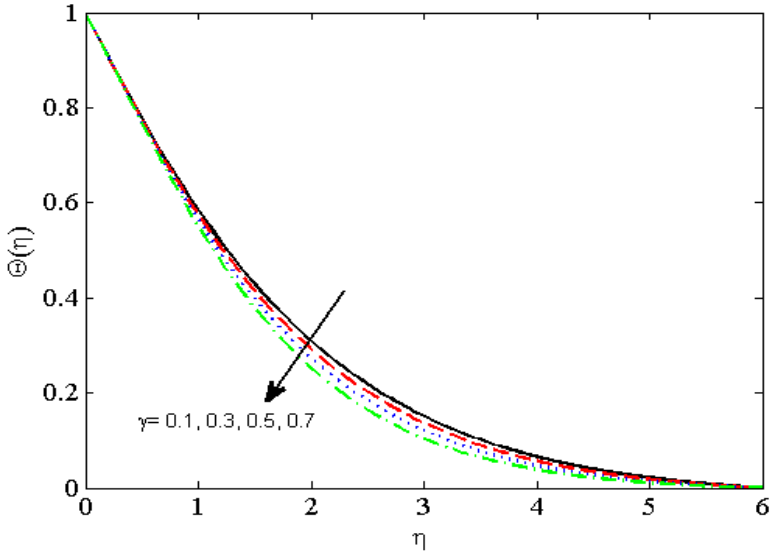

Fig. 15. Effect of γ on $\Theta(\eta)$.

the concentration. Fig. 14 demonstrates the effect of Deborah number (β) on $F'(\eta)$. Physically, Deborah number is proportional to the retardation time. Thus, an increment in the β causes to improves the retardation time. Accordingly, the fluid flow is accelerated.

Fig. 15 depicts the effect of thermal relaxation parameter (γ) on $\theta(\eta)$. It is clearly seen that the temperature decreases with the increase of γ. Physically, an enhancement in thermal relaxation parameter causes less heat transfer from sheet to the fluid. With this indication that the thermal boundary layer will be thinner when the relaxation time for heat flux is larger. Also, we conclude that the parameter γ behaves like a non-conductor. Fourier's Law can be deduced from the present model by applying $\gamma = 0$.

The numerical values of skin friction coefficient (Cf_x) and the rate of heat transfer and nanoparticle friction coefficients $(Nu_x,\ Sh_x)$ for different values of flow parameters are presented in Table 2. It is clear that Cf_x, Nu_x and Sh_x are decreasing functions of M and K. Due to the domination of opposing force, it is seen that an increase in M and Kdecreases the skin friction coefficient as well as the rate of heat and mass transfer coefficients. From this a conclusion has arrived that the magnetic field and porosity parameters are controlling the fluid flow. Also, the rising values of β and n enhances the skin friction coefficient. Whereas, it decreases with the improving values of α. Since the friction factor coefficient is proportional to flow velocity and wall thickness that tends to reduce the flow rate which causes the slower impact on sheet, hence the local skin friction coefficient decreases. The heat transfer rate (Nu_x) is decreases with the increasing values of β, γ, n, Nb and Nt but it accelerates with the enhancing values of α. Further, the improving values of β, n and Nt are decreases the nanoparticle friction factor coefficient (Sh_x). While the opposite

Table 1. Comparison of the numerical values of $-f''(0)$ for $\alpha = 0.5$ with $\lambda = M = Nt = Nb = R = Le = Kr = Ec = 0$, $K \to 0$.

n	Fang et al. [1]	Khader and Megahed [26]	Prasad et al. [10]	Present work
10.00	1.0603	1.0603	1.0605077120653874	1.060729
9.00	1.0589	1.0588	1.0511040757424492	1.059325
7.00	1.0550	1.0551	1.0552402381500168	1.055466
5.00	1.0486	1.0486	1.048791366557854	1.049050
3.00	1.0359	1.0358	1.035877993886442	1.036336
2.00	1.0234	1.0234	1.0230051676018523	1.023860
1.00	1.0000	1.0000	1.0	1.000483
0.50	0.9799	0.9798	0.9791336007879321	0.980384
0.00	0.9576	0.9577	0.9571649276940054	0.957924
-0.50	1.1667	1.1666	1.1668932098461453	1.666822

behavior is observed for the rising values of γ, Nb and α. However, γ, Nb and Nt show no effect on Cf_x.

Table 2. Numerical values of $F''(0)$, $-\Theta'(0)$ and $-\Phi'(0)$ when $\alpha = 0.5$, $\beta = 0.2$, $M = 0.5$, $\Pr = 0.71$, $\gamma = 0.2$, $\eta = 0.2$, $n = 0.5$, $\varepsilon_1 = 0.1$, $\varepsilon_2 = 0.1$, $Nt = 0.2$, $Nb = 0.3$, $Le = 2$, $K = 1.5$.

M	K	β	γ	n	Nb	Nt	α	$F''(0)$	$-\Theta'(0)$	$-\Phi'(0)$
1								-2.006454	0.318044	0.763048
2								-2.259932	0.305701	0.735526
3								-2.486737	0.296175	0.713085
	1							-1.714320	0.334895	0.798155
	2							-2.006454	0.318044	0.763048
	3							-2.259932	0.305701	0.735526
		0.1						-1.866680	0.325875	0.779685
		0.3						-1.865921	0.325629	0.779178
		0.5						-1.865184	0.325385	0.778670
			0.1					-1.866298	0.326759	0.779328
			0.3					-1.866298	0.324765	0.779514
			0.5					-1.866298	0.322858	0.779614
				1				-1.802472	0.270600	0.598693
				2				-1.770884	0.219415	0.431751
				3				-1.779541	0.194925	0.354747
					0.1			-1.866298	0.361013	0.474561
					0.2			-1.866298	0.342987	0.703590
					0.3			-1.866298	0.325752	0.779431
						0.1		-1.866298	0.334655	0.838556
						0.2		-1.866298	0.325752	0.779431
						0.3		-1.866298	0.317107	0.725338
							0.1	-1.729644	0.284225	0.645230
							0.3	-1.792975	0.304675	0.711716
							0.5	-1.866298	0.325752	0.779431

5 Final remarks

The hydromagnetic nanofluid flow over a stretching sheet through porous medium with variable wall thickness by using a new heat flux model namely, Cattaneo-Chirstov heat flux model is studied. The impact of various flow parameters on velocity, temperature and nanoparticle concentration as well as the friction factor coefficient, the rate of heat and mass transfer coefficients are derived and discussed through graphs and tables. The final remarks are

1. The friction factor coefficient is an increasing function of Deborah number and velocity index parameter.

2. A stronger magnetic field causes to increase the heat diffusion therefore; the heat transfer rate is decreases.

3. The enhancement of Le causes to decreases the Brownian diffusion coefficient. So, we noticed the reduction of nanoparticles concentration.

4. The larger value of the thermal relaxation parameter acts as non-conductor.

5. A greater value of wall thickness parameter leads to a large mass injection effect, which consequently enhances the fluid velocity while the opposite behavior is observed for mass suction effect.

References

[1] Fang, T., J. Zhang, Y. Zhong. Boundary Layer Flow over a Stretching Sheet with Variable Thickness. *Applied Mathematics and Computation*, **218** (2012), 7214-7252.

[2] Anjali Devi, S.P., M. Prakash. Temperature Dependent Viscosity and Thermal Conductivity Effects on Hydromagnetic Flow over a Slendering Stretching Sheet. *Journal of the Nigerian Mathematical Society*, **34** (2015), 318-330.

[3] Anjali Devi, S. P., M. Prakash. Thermal Radiation Effects on Hydromagnetic Flow over a Slendering Stretching Sheet. *Journal of the Brazilian Society of Mechanical Sciences and Engineering*, **38** (2016), 423-431. DOI 10.1007/s40430-015-0315-7.

[4] Anjali Devi, S. P., M. Prakash. Slip Flow Effects over Hydromagnetic Forced Convective Flow over a Slendering Stretching Sheet. *Journal of Applied Fluid Mechanics*, **9** (2016), 683-692.

[5] Vajravelu, K., K.V. Prasad, Hanumesh Vaidya. Influence of Hall Current on MHD Flow and Heat Transfer over a Slender Stretching Sheet in the Presence of Variable Fluid Properties. *Communications in Numerical Analysis*, **2016** (2016), 17-36.

[6] Hayat, T., I. Ullah, A. Alsaedi, M. Farooq. MHD Flow of Powell-Eyring Nanofluid over a Non-Linear Stretching Sheet with Variable Thickness. *Results in Physics*, **7** (2017), 189-196.

[7] HAYAT, T., M. WAQAS, A. ALSAEDI, G. BASHIR, F. ALZAHRANI. Magnetohydrodynamic (MHD) Stretched Flow of Tangent Hyperbolic Nanoliquid with Variable Thickness. *Journal of Molecular Liquids*, **229** (2017), 178-184.

[8] KIRAN KUMAR, R. V. M. S. S., S. V. K. VARMA. Hydromagnetic Boundary Layer Slip Flow of Nanofluid through Porous Medium over a Slendering Stretching Sheet. *Journal of Nanofluids*, **6** (2017), 852-861. DOI 10.1166/jon.2017.1386.

[9] KIRAN KUMAR, R. V. M. S. S., S. VIJAYA KUMAR VARMA, C. S. K. RAJU, S. M. IBRAHIM, G. LORENZINIAND E. LORENZINI. Magnetohydrodynamic 3D Slip Flow in a Suspension of Carbon Nanotubes over a Slendering Sheet with Heat Source/Sink. *Continuum Mechanics and Thermodynamics*, **29** (2017), 835-851. DOI 10.1007/s00161-017-0563-0.

[10] PRASAD, K.V., K. VAJRAVELU, HANUMESH VAIDYA, R. A. VAN GORDER. MHD Flow and Heat Transfer in a Nanofluid over a Slender Elastic Sheet with Variable Thickness. *Results in Physics* **7** (2017), 1462-1474.

[11] FOURIER, J. B. J. Theorieanalytique De La chaleur, Paris, 1822.

[12] CATTANEO, C. Sulla conduzione del calore. *Atti Semin. Mat. Fis. Univ. Modena Reggio Emilia*, **3** (1948), 83-101.

[13] CHRISTOV, C. I. On Frame Indifferent Formulation of the Maxwell–Cattaneo Model of Finite Speed Heat Conduction. *Mechanics Research Communications*, **36** (2009), 481-486.

[14] TIBULLO, V., V. ZAMPOLI. A Uniqueness Result for the Cattaneo–Chirstov Heat Conduction Model Applied to Incompressible Fluids. *Mechanics Research Communications*, **38** (2011), 77-79.

[15] HAN, S., L. ZHENG, C. LI, X. ZHANG. Coupled Flow and Heat Transfer in Viscoelastic Fluid with Cattaneo–Christov Heat Flux Model. *Applied Mathematics Letters*, **38** (2014), 87-93.

[16] SHAHID, A., M. M. BHATTI, O. ANWAR BG, A. KADIR. Numerical Study of Radiative Maxwell Viscoelastic Magnetized Flow from a Stretching Permeable Sheet with the Cattaneo–Christov Heat Flux Model. *Neural Computing & Applications*, March (2017), 1-12. DOI 10.1007/s00521-017-2933-8.

[17] MUSTAFA, M. Cattaneo–Christov Heat Flux Model for Rotating Flow and Heat Transfer of Upper Convected Maxwell Fluid. *AIP Advances*, **5** (2015), 047109.

[18] SALAHUDDIN, T., M. Y. MALIK, ARIF HUSSAIN, S. BILAL, M. AWAIS. MHD Flow of Cattaneo–Christov Heat Flux Model for Williamson Fluid over a Stretching Sheet with Variable Thickness: Using Numerical Approach. *Journal of Magnetism and Magnetic Materials*, **401** (2016), 991-997.

[19] DOGONCH, A. S., D. D. GANJI. Impact of Cattaneo–Christov Heat Flux on MHD Nanofluid Flow and Heat Transfer between Parallel Plates Considering Thermal Radiation Effect. *Journal of the Taiwan Institute of Chemical Engineers*, **000** (2017), 1-12.

[20] HAYAT, T., A. KIRAN, M. IMTIAZ, A. ALSAEDI. Unsteady Flow of Carbon Nanotubes with Chemical Reaction and Cattaneo–Christov Heat Flux Model. *Results in Physics*, **7** (2017), 823-831.

[21] AHMAD KHAN, J., M. MUSTAFA, T. HAYAT, A. ALSAEDI. Numerical Study of Cattaneo-Chirstov Heat Flux Model for Visco-Elastic Flow Due to an Exponentially Stretching Surface. *PLoS ONE*, **10** (2015). DOI 10.1371/journal.pone.0137363.

[22] STRAUGHAN, B. Thermal Convection with the Cattaneo–Christov Model. *International Journal of Heat and Mass Transfer*, **53** (2010), 95-98.

[23] RUBAB, K., M. MUSTAFA. Cattaneo-Christov Heat Flux Model for MHD ThreeDimensional Flow of Maxwell Fluid over a Stretching Sheet. *PLoS ONE*, **11** (2016), e0153481. DOI 10.1371/ journal.pone.0153481.

[24] MALIK, M.Y., MAIR KHAN, T. SALAHUDDIN, IMAD KHAN. Variable Viscosity and MHD Flow in Casson Fluid with Cattaneo–Christov Heat Flux Model: Using Keller Box Method. *Engineering Science and Technology, an International Journal*, **19** (2016), 1985-1992.

[25] HAYAT, T., M. FAROOQ, A. ALSAEDI, FALLEH AL-SOLAMY. Impact of Cattaneo–Christov Heat Flux in the Flow over a Stretching Sheet with Variable Thickness. *AIP Advances*, **5** (2015), 1-12.

[26] KHADER, M. M., AHMED M. MEGAHED. Numerical Solution for Boundary Layer Flow Due to a Nonlinearly Stretching Sheet with Variable Thickness and Slip Velocity. *European Physical Journal - Plus*, **128** (2013), 100. DOI 10.1140/epjp/i2013-13100-7.

[27] HAYAT, T., M.S. ANWAR, M. FAROOQ, A. ALSAEDI. Mixed Convection Flow of Viscoelastic Fluid by a Stretching Cylinder with Heat Transfer. *PloS ONE*, **10** (2015), 1-20.

[28] KUZNETSOV, A. V., D. A. NIELD. The Cheng–Minkowycz Problem for the Double-Diffusive Natural Convective Boundary Layer Flow in a Porous Medium Saturated by a Nanofluid. *International Journal of Heat and Mass Transfer*, **54** (2011), 374-378.

[29] FARID, M. M. Mathematical Modeling of Food Processing, CRC Press, 2010, pp. 38-39.

[30] KLEINSTREUER, C. Engineering Fluid Dynamics: An Interdisciplinary Systems Approach, Cambridge University Press, 2005.

APPENDIX

$$\alpha = A\sqrt{\frac{U_0(n+1)}{2\upsilon}}\,, \qquad \eta = \alpha = A\sqrt{\frac{U_0(n+1)}{2\upsilon}}\,, \qquad \Pr = \frac{\upsilon}{\alpha}\,,$$

$$Le = \frac{\nu}{D_B}\,, \qquad Nb = \frac{\tau D_{B\infty}(C_w - C_\infty)}{\upsilon}\,, \qquad Nt = \frac{\tau D_T(T_w - T_\infty)}{T_\infty \upsilon}\,,$$

$$M = \frac{2\sigma B_0^2}{U_0(n+1)\rho}\,, \qquad K = \frac{U_0(1+n)k'}{2\upsilon}\,,$$

$$\beta = \lambda_1 U_0 (x+b)^{n-1}\,, \qquad \gamma = \lambda_2 U_0 (x+b)^{n-1}\,.$$